Original article

Institution of MECHANICAL ENGINEERS
Journal of MATERIALS: DESIGN AND APPLICATIONS

Proc IMechE Part L:
J Materials: Design and Applications
0(0) 1–9

DOI: 10.1177/1464420718809502
journals.sagepub.com/home/pil
SAGE

Fatigue-induced dual stiffness behavior of filled styrene–butadiene rubber

Ruofan Liu and Erol Sancaktar

Abstract

Payne and Mullins effects are widely observed in reinforced rubber materials. The mechanisms by which these two effects work are not fully understood. Several models have been proposed, including molecular slippage model, bond rupture model, and filler rupture model. In this study, two different compounds of styrene–butadiene rubber were prepared using carbon black and silica as reinforcement fillers, respectively, and subjected to cyclic fatigue process. Tensile, creep, and relaxation tests were performed on fatigued samples to assess the residual stress–strain behavior by comparing with the results from similar tests using pristine (no fatigue) samples. When the tensile stiffness behavior of fatigued specimens was evaluated, we noted that the stiffness versus strain behavior which exhibited a monotonic decreasing–increasing behavior with the pristine specimens changed to what we call "dual-stiffness" condition, where the specimens went through a first (low) turning point as with the pristine samples, but then dropped off of a peak to go through a second softening stage, similar to the first softening stage of the pristine material. We believe that such spiking (dual) stiffness behavior characterized by a "Peak" point represents a combination of both Payne and the Mullins effects active during fatigue loading. We conclude that molecular slippage and bond rupture are the main factors affecting the physical properties of carbon black-filled compounds, while breakage and recombination of the filler are the key mechanisms affecting the silica-filled compounds during the fatigue process.

Keywords

Styrene–butadiene rubber, fatigue, Payne effect and Mullins effect, residual stress–strain behavior, creep and relaxation

Date received: 13 June 2018; accepted: 5 October 2018

Introduction

Rubbers are widely used in industrial applications because of their unique mechanical properties.[1,2] During service, rubber parts are often subjected to cyclic loading conditions such as tires being subjected to cyclic load during operation.

The Payne and Mullins effects are two particular features of the stress–strain behaviors of rubber compounds containing fillers. The Payne effect demonstrates a dependence of the viscoelastic storage modulus (G′) on the amplitude of the applied strain under dynamic strain sweep conditions. When the strain amplitude is small (~0.1%), G′ decreases rapidly with increasing strain level. As the strain amplitude continues to increase, G′ typically reaches the lowest level, while the loss modulus, G″, shows a maximum in that strain amplitude region.

The Mullins effect focuses on the stress–strain behavior of vulcanized rubber under large strain amplitude cyclic loads. If a piece of vulcanized rubber is stretched and the load released subsequently, it will not exhibit the same stress–strain curve when it is stretched once again up to the previously reached elongation level. The stress–strain curve shifts down in comparison to the original curve. When the subsequent strain amplitudes exceed the level prior to unloading, the stress–strain curve then reaches and follows the same (previous) curve for the unloaded cycle.

Numerous studies have been performed on the Payne and Mullins effects using both experimental and theoretical approaches.[3–12] Many models have been proposed to explain the physical phenomena observed. Some researches focused on small shear rate and small oscillation amplitude (smaller or around 1%) and found that the Payne effect is a purely strain rate-dependent phenomenon, and strain sequence-dependent dynamic behavior changes (rather than Mullins effect) taking place.[10,11] Also, some rubber professionals attribute the Payne effect

Polymer Engineering Department, The University of Akron, Akron, USA

Corresponding author:
Erol Sancaktar, University of Akron, 250 S. Forge St., Akron, OH 44325-0301, USA.
Email: erol@uakron.edu

to filler–filler interactions and the Mullins effect to filler–rubber interactions. Nevertheless, these two effects have not been fully understood.

Researches on the fatigue behavior of rubber materials have been carried out for a long time.[13–27] Many rubber formulations and compounds have been studied. Polymer types, filler types, and types of other compounded ingredients (i.e. vulcanizing agents, antioxidants, etc.) are considered the main factors influencing the fatigue behavior. The manufacturing processes are also considered to influence the fatigue behavior since they determine the dispersion of fillers in the rubber. Crosslink density determines the physical properties to a large degree.[23,28] Usually, high crosslink density relates to high stiffness and low level of hysteresis. Crosslink density also relates to viscoelastic properties of rubbers.[23,29–32] Creep rate drops dramatically with increasing crosslink density at low levels and then the creep curve levels off. The creep rate in total depends on the rubber type, the filler dose, and the vulcanization system. Stress relaxation rates exhibit similar results.

In our study, we used a residual stress–strain behavior method as related to the Payne and Mullins effects. For this purpose, we prepared two different compounds of styrene–butadiene rubber (SBR) using carbon black and silica as reinforcement fillers, respectively, and subjected these compounds to cyclic fatigue loadings. Tensile, creep, and relaxation tests were performed on fatigued samples to assess the residual stress–strain behavior by comparing with the results from similar tests using pristine (no fatigue) samples. When the tensile stiffness behavior of fatigued specimens were evaluated, it was noted that the stiffness versus strain behavior exhibited a ''dual-stiffness'' condition, where the specimens went through a first (low) turning point as with the pristine samples, but then dropped off of a peak to go through a second softening stage, similar to the first softening stage of the pristine material. We believe that such spiking (dual) stiffness behavior characterized by a ''Peak'' point represents a combination of both Payne and Mullins effects. The dual-stiffness behavior is utilized subsequently to relate stiffness changes in silica-filled compound to the silica filler's agglomerate breakup and reagglomeration behavior. Creep and relaxation tests results support the idea that the rubber crosslinks in the silica-filled compound do not fail to a large extent during fatigue loading thus providing further evidence of filler–filler agglomerate-dominated stress–strain behavior for the silica-filled rubber compound.

Experiments

Materials and specimen preparations

Formulations of compounds. In this project, we used SBR as the base material. SBR is widely used in tire industries. In order to obtain a clear picture of how various filler particles will influence the fatigue performance of the rubber, two SBR compounds were used. The compound formulations are shown in Table 1 in phr form with the main difference between the two compounds being the reinforcement fillers. One of the compounds was filled with carbon black and the other one was filled mainly with silica particles. The rest of the formulations for these two compounds, including the rubber material were basically the same. These compounds were prepared by Cabot. Co. (Billerica, MA).

Dumbbell specimen vulcanization and preparation. ASTM D4482 standard was used to prepare dumbbell specimens. The cure temperature was 160 °C (320 °F) and the cure pressure was 15 MPa (2200 psi). The vulcanization times were determined by using rubber process analyzer (RPA) (RPA 2000, Alpha technology, Akron, OH) corresponding to 90% cure, which in this case were 11 min for carbon black-filled compound and 40 min for silica-filled compound, respectively. The specimens were cured in a rectangular mold made specially to conform to the fatigue tester discussed in the following section.

After the curing process, specimens were cut into dumbbell strips following the ASTM D4482 standard. Geometrical parameters of the specimens, except the thicknesses, are shown in Figure 1. As can be seen, these specimens had cylindrical flanges at their gripping ends to slide into the loading grips of the fatigue tester. The thicknesses of the specimens fluctuated from 1.4 to 1.6 mm.

Fatigue test

A Dynisco Fatigue to Failure instrument (Franklin, MA) was used to run fatigue tests. It operates based on ASTM D4482 test standard using dumbbell specimens. The fatigue instrument is displacement controlled, and the displacements can be converted into

Table 1. Formulations of styrene–butadiene rubber (SBR) compounds used.

	Silica filled	Carbon black filled
Buna VSL 4720-0 HM	100	100
Z1165 SILICA	50	
N234 carbon black		50
Vulcan 3 carbon black	4	
SI 69	4	
Zinc oxide RGT-M	3	3
Stearic acid rubber grade	2	2
Standard 6PPD	1	1
CBTS accelerator	1.5	1.4
Sulfur	1.6	1.6

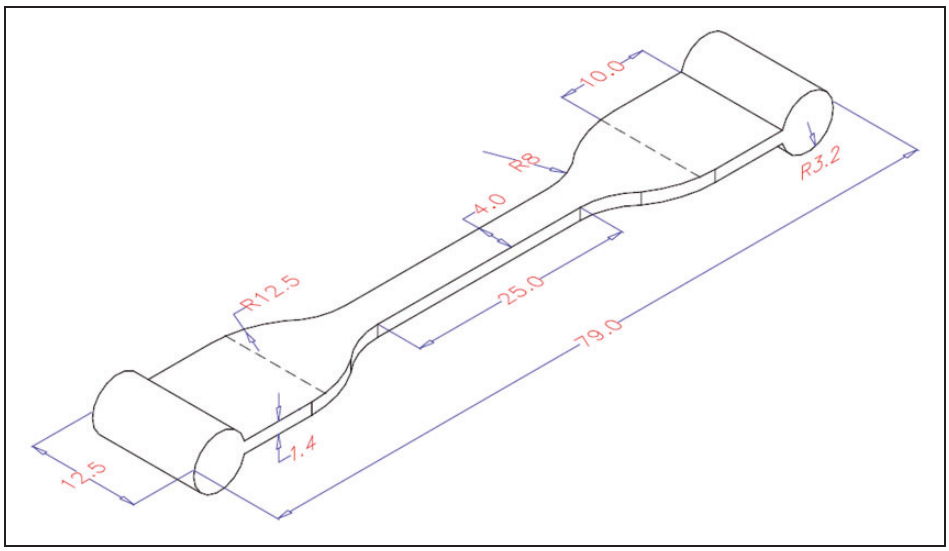

Figure 1. Dumbbell specimen sketch and parameters based on ASTM D4482 standard.

strain levels as described by the ASTM D4482 standard. The strain levels can be chosen from 61 to 136%. In this project, 61 and 101% strain amplitudes were chosen with 61% estimated as the closest strain value encountered during tire operation. The cyclic loading was in "repeated" pattern. The frequency was fixed at 1.7 Hz (100 cycles/min). If the specimens reached a predetermined fatigue level without failure, the specimen would be taken out of the fatigue tester and subjected to subsequent tests. A computer control was provided with the instrument to monitor the number of cycles applied, including cycles at failure, as well as the ability to set a specific number of cycles to be applied. There were some cracks which could be observed through micro-CT scan in the surviving samples. However, those cracks did not lead to catastrophic failure. Furthermore, the dimensional changes were not serious in those samples.[33–35]

Tensile and viscoelastic properties tests

An Instron 5567 tensile tester (Norwood, MA) was used to run constant crosshead rate tensile tests. Since rubbers exhibit rate-dependent viscoelastic properties, two crosshead rates, 5 and 500 mm/min were chosen. The strain values were converted from extension data collected by the Instron tensile system.

Relaxation and creep tests were also performed using the Instron 5567 tensile tester to study viscoelastic properties of the fatigued rubber compounds. The comparisons among various fatigue level specimens provided a method to access rubber materials' residual viscoelastic behavior.

Twelve-hour, 61% strain amplitude relaxation test was applied to both pristine and fatigued specimens of carbon black- and silica-filled compounds. In order to maintain similar conditions, the applied creep stress was estimated from the tensile test data by converting strain amplitude into stress using pristine specimen's 500 mm/min crosshead rate stress–strain curve. Due to the stress–strain curve differences between the carbon black- and silica-filled compounds, the creep stress values used for carbon black-filled compounds and for silica-filled compounds were not the same. Stress levels for each compound are presented in Table 2. Other experimental conditions for the creep test were similar to the relaxation test. Twelve-hour creep tests were performed with both pristine and fatigued samples.

Table 2. Stresses used in creep test for each compound.

	Carbon black-filled compound (MPa)	Silica-filled compound (MPa)
Corresponding to 61% strain	2.65	2.68

The initial creep rates and the asymptotic values of relaxation tests were calculated by using the first half hour and last half hour of the experiments, respectively. The asymptotic relaxation values were calculated as the average stress values observed during the last half hour of the relaxation tests.

Results and discussion

Fatigue tests

During the fatigue tests, most of the samples did not survive to specific cycle numbers we set. Our overall test results revealed that the fatigue to failure cycle numbers were affected by compounding, filler type, filler dispersion, and fatigue strain amplitude.

For example, with CB-filled specimens loaded to 61% strain amplitude, about 50% of the specimens failed at each million cycles applied. Only 39.58% of the initially pristine samples survived two million fatigue cycles, and only 16.49% of the initially pristine

specimens survived three million fatigue cycles. At higher strain amplitudes, fatigue to failure cycle numbers dropped significantly, i.e. all specimens would fail after a few thousand fatigue cycles if the fatigue strain amplitude was set to 101%. Obviously, specimens containing initial defects such as large voids and large agglomerates of fillers would fail rather quickly under catastrophic crack propagation without achieving the full potential of the rubber compound. The presence of such defects was verified using CT scan (SkyScan 1172, Kontich, Belgium) with several specimens during various stages of fatigue loading as reported in our previous articles.[33–35] We would like to note, therefore, that the results we report in the subsequent sections of this work thus provide highly reliable basis for our discussions on Payne and Mullins effects from a constitutive (continuum mechanics) point of view as they represent the behavior of rubber compounds realizing their full material potential observed with pristine (no fatigue specimens) rather than failing prematurely and catastrophically.

Observation of Payne and Mullins effects: Dual-stiffness behavior

Tangent stiffness at each strain point was calculated as the first derivative of stress w.r.t. strain [$\sigma'(\epsilon)$]. Representative figures for the variation of moduli with strain are shown in Figure 2 for the pristine and fatigued specimens.

The effect of cyclic loading on stiffness was evaluated by comparisons throughout tensile testing. The data presented in this section were obtained using 61% fatigue strain amplitude and pristine specimens of both carbon black- and silica-filled compounds.

When evaluating the stiffness behavior of fatigued specimens, it was noted that the stiffness versus strain behavior which exhibited a monotonic decreasing–increasing behavior with the pristine specimens (Figure 2) changed to ''dual-stiffness'' condition, where the specimens went through a first (low) turning point as with the pristine samples, but then dropped off of a peak to go through a second softening stage, similar to the first softening stage of the pristine material, as shown in Figures 2 to 4. The samples then start a second strain-stiffen stage and reach lower stiffness levels in comparison to the pristine sample. These ''threshold'' points were named ''Max,'' ''Turning Point 1 (TP1),'' ''Peak,'' and ''Turning Point 2 (TP2)'' as shown in Figure 3.

The ''dual-stiffness'' plot shown in Figure 5(a) was obtained using carbon black-filled SBR, fatigued using two million cycles, and the crosshead rate was 5 mm/min. Silica-filled samples typically failed at much lower numbers of fatigue cycles.

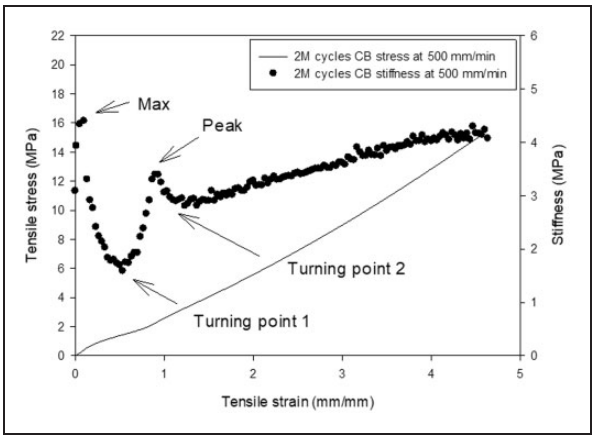

Figure 3. Typical ''dual-stiffness'' behavior in fatigued samples with characterizing threshold points, ''max,'' ''Turning Point 1,'' ''Peak,'' and ''Turning Point 2'' marked. The data shown corresponds to carbon black-filled SBR, fatigued using two million cycles and subsequently tested in tension at 500 mm/min.
CB: carbon black.

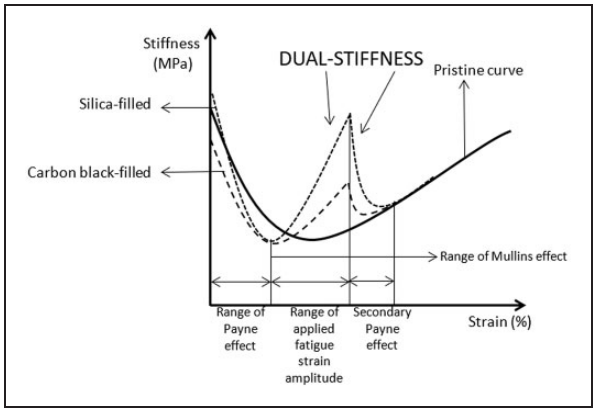

Figure 2. Illustrations of variations in pristine stiffness and fatigued specimens' dual-stiffness modulus curves with the level of strain.

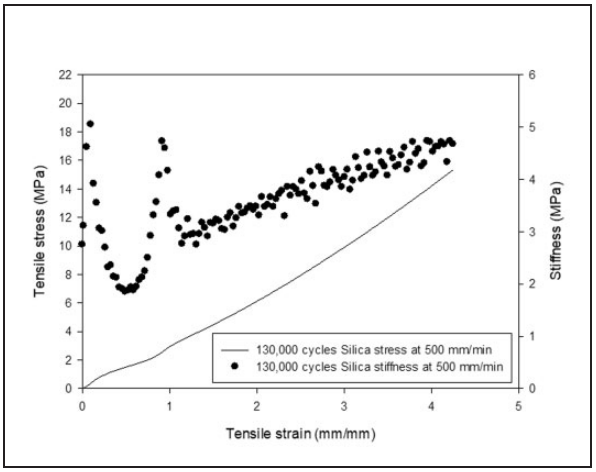

Figure 4. ''Dual-stiffness'' behavior in silica-filled SBR samples fatigued using 130,000 cycles and subsequently tested in tension at 500 mm/min.

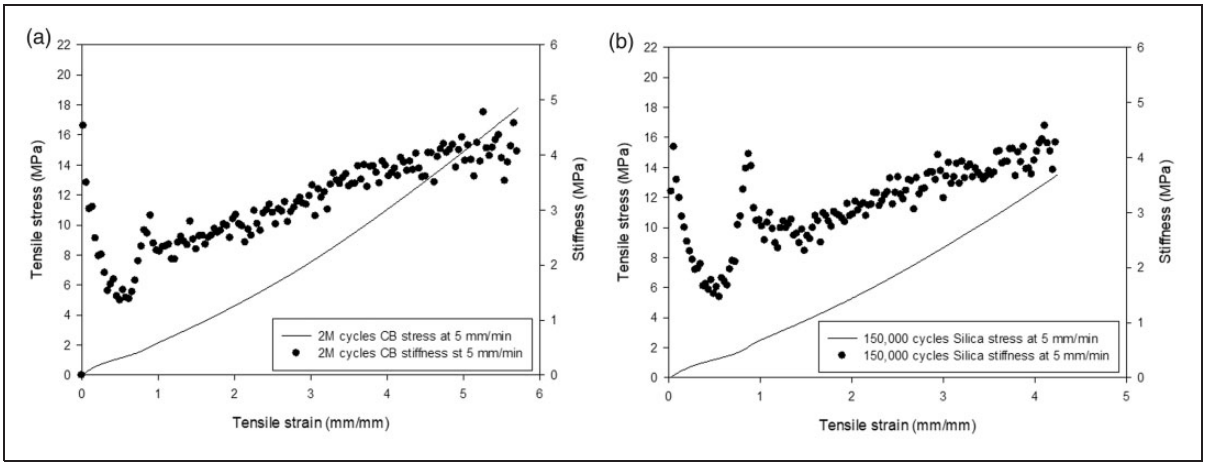

Figure 5. Examples of duality in stiffness as measured by stiffness variation during tensile tests at 5 mm/min for carbon black-filled compound fatigued two million cycles (a), and silica-filled compounds fatigued 150,000 cycles (b).

Consequently, "dual-stiffness" plot shown in Figure 5(b) represents silica-filled compounds fatigued using 150,000 cycles, and the crosshead rate was 5 mm/min. The stress–strain curves for the two compounds exhibit very similar behavior when the fatigued samples were tested subsequently under tensile test at 5 mm/min (Figure 5).

Comparison of Figures 4 and 5 reveals that, even though the silica-filled specimens exhibit higher stiffness values in comparison to the carbon black-filled ones up to the "Peak" stiffness point, beyond that point, stiffness falls to levels similar to those with carbon black. After the breakage of silica filler aggregation during the fatigue process, the silica particles would have redispersion in the rubber. Such redispersion generates new connections between the fillers or between the fillers and rubber. Those connections made the stiffness "Peak" of silica-filled compound reach or even exceed the "Max" point in the stiffness curves.

We believe that such spiking stiffness behavior is a combination of both the Payne effect and the Mullins effect. It represents attempts by the fatigue-damaged material to strain stiffen in a manner similar to the pristine version. The stiffness "Peaks" show up right after strain amplitudes used during the fatigue tests falling somewhere between the "Turning Point 1" and the "Peak" point. We note that the slope of the stress–strain curve (i.e. the stiffness) is higher than that of the pristine material when it is tending to merge with the pristine stress–strain curve during the reloading (i.e. tensile testing) process (see Figure 6).

Based on the Mullins effect, once the rubber compounds are subjected to cyclic loads, we expect the stress–strain curves from the subsequent tensile tests to be lower than those for the pristine compounds until the strain amplitudes of the fatigue tests are reached (Figure 6). If the fatigued samples are subsequently stressed in an increasing fashion (during tensile testing) to make the strain amplitude exceed the

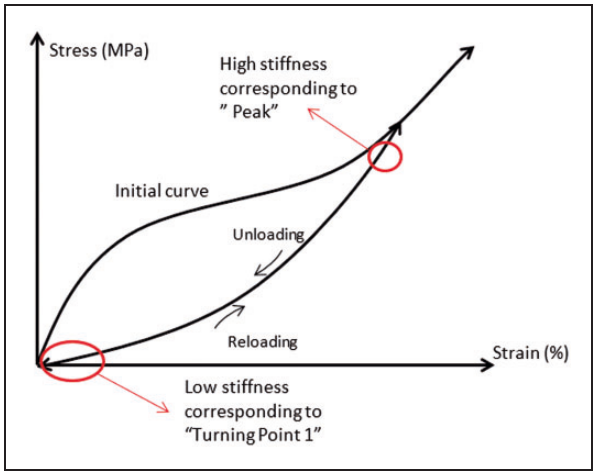

Figure 6. Illustration of Mullins effect.

previously applied value under cyclic condition, the stress–strain curve is expected to merge with the stress–strain curve for the pristine sample. Since curves for the fatigued samples would "catch up with" the pristine sample curves, there must be a high stiffness region when the strain amplitude exceeds the fatigue strain. The stiffness range between the "Turning Point 1" and the "Peak" point represents this high stiffness region in tensile stress–strain curves. However, the fatigue-damaged material is not able to strain stiffen beyond the "Peak" point due to morphological changes occurring by cycling and due to filler–filler interactional changes by a "Secondary Payne Effect" (see Figure 3).

Threshold points for stiffness values of the compounds' fatigued samples at two crosshead rates (5 and 500 mm/min) are shown in Figure 7. In these figures, the values reported for the pristine samples at "Peak" and "Turning Point 2" correspond to their moduli at the "Peak" and "Turning Point 2" strain levels of the fatigued samples. The numbers above the bars represent the strain levels at the threshold points.

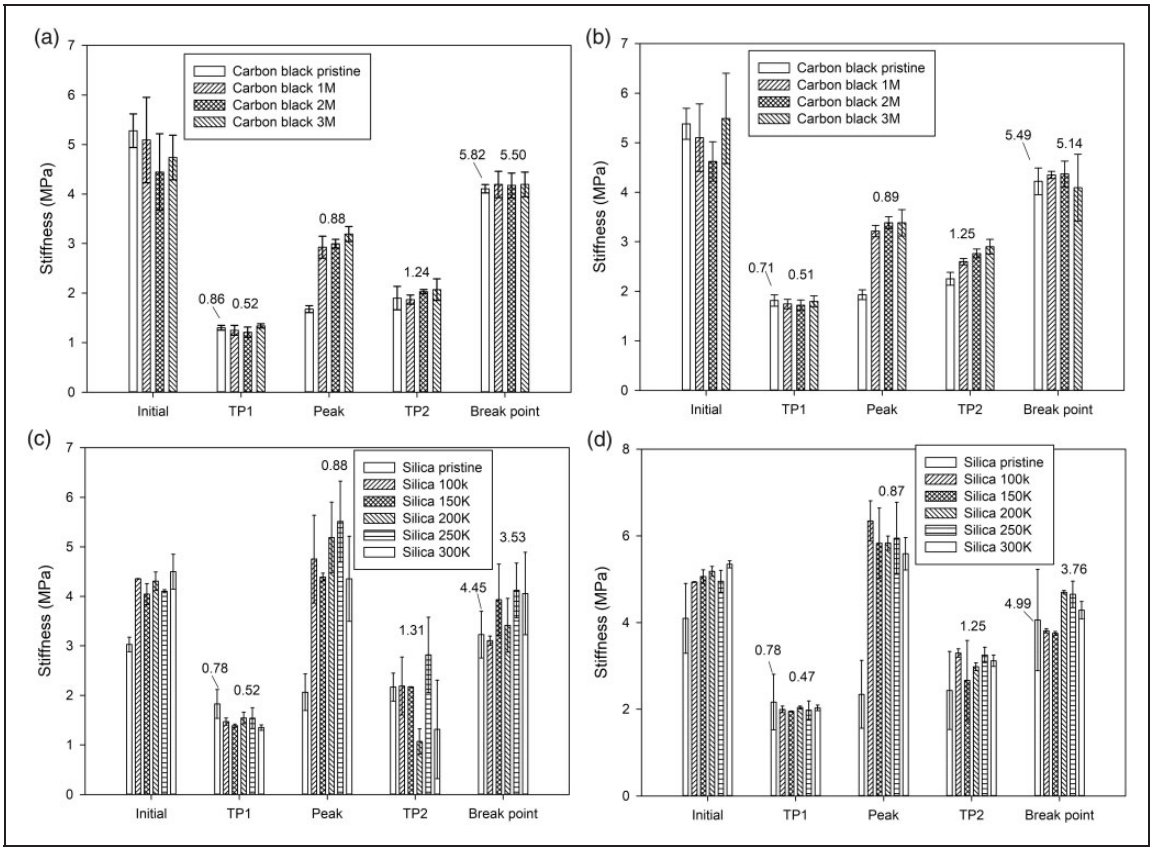

Figure 7. Threshold points for stiffness values and strain values of two compounds' fatigued samples subsequently tested at 5 and 500 mm/min tensile crosshead rates. The moduli values of pristine samples at "Peak" and "Turning Point 2" are the corresponding moduli values of pristine samples at the strain levels which are averages of fatigued samples at their peak and Turning Point 2: (a) carbon black-filled compound at 5 mm/min crosshead rate, (b) carbon black-filled compound at 500 mm/min crosshead rate, (c) silica-filled compound at 5 mm/min crosshead rate, and (d) silica-filled compound at 500 mm/min crosshead rate.
TP1: Turning Point 1; TP2: Turning Point 2.

When the specimens were subjected to fatigue loading, "Turning Point 1" showed up at a low strain level, as it did for the pristine samples (i.e. the Payne effect). Stiffness values at "Turning Point 1" of fatigued specimens are similar to the pristine specimens for carbon black-filled compound and a little lower than pristine sample values for the silica-filled compound. This observation reveals that more serious interfacial or structural changes were taking place as a result of the fatigue process in the silica-filled compounds than the carbon black-filled compounds. The reason could be the breakage of silica filler agglomerations. Agglomerated carbon black and silica particles contained in rubber would increase the modulus of the material, such reinforcement depending on the specific surface and volume fractions of the reinforcement.[36] Fatigue process cannot change the molecular structures, bonds, and volume fractions of the filler; thus, the stiffness values at "Max" and "Turning Point 1" do not change much when the specimens are subjected to fatigue. During any extensional process, some filler agglomerations are expected to break up, leading to local filler dispersion changes, such as breakage and recombination of hydrogen bonds and Van der Waals forces. Such changes may cause the early coming of minimum stiffness value at low strain amplitude. As shown in Figure 6, the "Peak" stiffness values of carbon black compound were lower than the "Max" stiffness values, while those values for the silica compound were greater than the original values. This is possibly caused by morphological rearrangements of silica. Silica fillers have more agglomerations in comparison to carbon black fillers, due to a larger amount of hydroxyls presence. Hydroxyls make it easier for the silica filler to form hydrogen bonds than the carbon black filler. This leads to conditions conducive to filler agglomeration in silica-filled compounds. Thus, subsequent to the breakage of agglomerations of silica filler during the initial straining process (Payne effect), recombination and dispersion changes of the silica filler are expected to take place during the cyclic loading. Such recombination increases the load-hold capability of the silica-filled compound, making the "Peak" stiffness values greater than its "Max" values. For most samples and starting with the "Peak" point, the stiffness values for fatigued samples are generally higher than the corresponding pristine values due to strain stiffen. Moreover, for most silica-filled specimens, in general, the second turning points

representing the end of the "Secondary Payne Effect" are higher than the first turning points representing the end of primary (initial) Payne effect, possibly due to morphological rearrangements (reduced chemical bonds in all samples, and agglomerate breakup/particle redistribution in silica systems).

For the carbon black system, the break point stiffness values are generally lower than the maximum stiffness values (Figure 7(a) and (b)); for the silica system tested at 5 mm/min rate, however, those two values are fairly close (Figure 7(c)). This observation may point out to weak interfacial forces between the silica particles and the SBR rubber, which do not seem to contribute as much to the compound stiffness neither at initial nor at the break loading points. When tested at the higher speed of 500 mm/min, the silica system shows higher stiffness initially, due to the viscoelastic behavior of SBR rubber (Figure 7(d)). In both tensile speeds, the break point strains of pristine samples are greater than the fatigued samples, indicating that cracks (tears) develop with the application of cyclic fatigue loads.

Fatigue cycle-dependent variability in stiffness values for the silica system (Figure 7(c) and (d)) seems to be much higher than that with the carbon black system (Figure 7(a) and (b)), possibly due to the issues related to breakage and recombination of silica agglomeration.

Viscoelastic behavior of the rubber compounds

Creep and relaxation rates of thermoset or vulcanized polymer materials are influenced by their crosslink density.[15] Generally, creep rate is inversely proportional to the crosslink density. In order to obtain the viscoelastic properties of our rubber compounds, creep and relaxation tests were performed by using Instron tensile tester and the initial creep rates (creep rates of initial half hour) and the asymptotic relaxation levels were calculated. The fatigued samples used in creep and relaxation tests were those which survived the 61% strain amplitude fatigue tests at several fatigue cycle levels. The plots of initial creep rate versus fatigue cycles and the asymptotic relaxation stress versus fatigue cycles are shown in Figure 8 for carbon black- as well as silica-filled compounds. The initial creep rates were calculated by using the first half hour data of the experiments, which represents the rapid (primary) creep stage. The asymptotic values of relaxation stress were calculated by using the last half hour data of the experiments.

Figure 8(a) reveals that, as the cycle numbers increase, the initial creep rate increases for the carbon black compound. The initial creep rate for the silica-filled compound, however, seems to be independent of the number of fatigue cycles. Since the creep rate reflects the crosslink density of rubber, increasing of the creep rate in carbon black compound points to breakage of its crosslink structure; while for the silica-filled compound, increasing fatigue cycles do not seem to influence its crosslink density. Asymptotic relaxation values of silica compound decreased with increasing fatigue cycles, possibly due to the development of cracks during the fatigue process. The asymptotic relaxation values for the carbon black compound, however, changed little, possibly due to less amount of crack formation. Cracks develop in silica-filled compounds faster and more prominently during the fatigue process. This behavior was verified by our microscopy and CT scan results in our previously published articles.[33,35] Cracks lead to a higher failure percentage and smaller break strain amplitudes (Figure 7) compared with the carbon black compound, as discussed in previous sections. Since moduli of the silica compound are higher than those of the carbon black compound, the asymptotic relaxation values of the silica compound are greater than those of the carbon black compound.

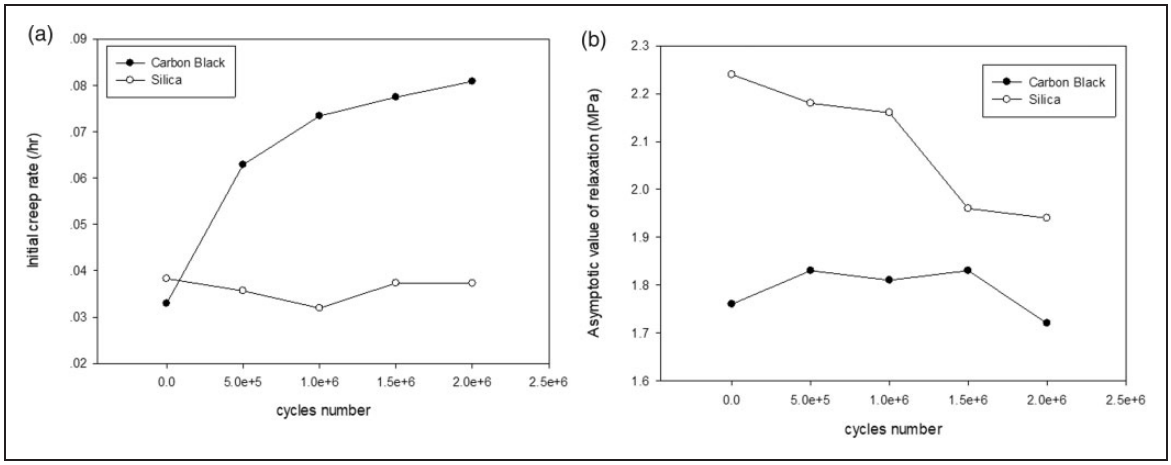

Figure 8. The effects of fatigue cycles on initial creep rate (a) and asymptotic values of relaxation stress (b) for CB-filled and SF compounds under 61% strain amplitude.

Conclusions

Payne and Mullins effects were observed by testing carbon black- and silica-filled SBR compounds under fatigue and subsequent monotonic tensile loadings to obtain their residual stress–strain behavior. It was shown that as the number of fatigue cycles accumulated, the percentages of the failed samples increased during the fatigue process. This revealed that cracks developed in both the carbon black- and silica-filled compounds with increasing fatigue cycles. Stiffness curves showed that the initially applied fatigue loading caused the stiffness to decrease quickly in carbon black-filled compound, pointing to chemical bonds rupture and molecular slippage processes. But, these mechanisms did not seem to be effective for the silica-filled compound. When we evaluated the stiffness behavior of fatigued specimens, we noted that the stiffness versus strain behavior which exhibited a monotonic decreasing–increasing behavior with the pristine specimens changed to what we call ''dual-stiffness'' condition, where the specimens went through a first (low) turning point (''Turning Point 1'') as with the pristine samples, but then dropped off of a peak to go through a second softening stage, similar to the first softening stage of the pristine material. We believe that such spiking (dual) stiffness behavior characterized by the ''Peak'' point represents a combination of both Payne and the Mullins effects. Dual-stiffness behavior reveals that the stiffness changes in silica-filled compound are related to the silica filler's agglomerate breakup and reagglomeration behavior. Stiffness ''Peak'' values of silica-filled compound are greater than its beginning (''Max'') values, revealing that recombination of silica particles is taking place during the fatigue process. The recombination of silica fillers could be caused by Van der Waals forces and hydrogen bonds, but further studies are needed to fully understand the mechanisms of filler recombination. Results from our creep and relaxation tests also support the idea that the rubber crosslinks in the silica-filled compound do not fail to a large extent during fatigue loading.

Declaration of conflicting interests

The author(s) declared no potential conflicts of interest with respect to the research, authorship, and/or publication of this article.

Funding

The author(s) disclosed receipt of the following financial support for the research, authorship, and/or publication of this article: Financial support by Center for Tire Research (CenTire), an NSF Industry/University Cooperative Research Center at Virginia Tech and The University of Akron, equipment support by the University of Akron Applied Polymer Research Center (APRC) are gratefully acknowledged.

ORCID iD

Erol Sancaktar http://orcid.org/0000-0003-0165-587X

References

1. Woo C-S, Kim W-D and Kwon J-D. A study on the material properties and fatigue life prediction of natural rubber component. *Mater Sci Eng A* 2008; 483–484: 376–381.
2. Le Cam J-B, Huneau B and Verron E. Description of fatigue damage in carbon black filled natural rubber. *Fatigue Fract Eng Mater Struct* 2008; 31: 1031–1038.
3. Mars WV. Evaluation of a pseudo-elastic model for the Mullins effect. *Tire Sci Technol* 2004; 32: 120–145.
4. Harbour R, Fatemi A and Mars W. Fatigue life analysis and predictions for NR and SBR under variable amplitude and multiaxial loading conditions. *Int J Fatigue* 2008; 30: 1231–1247.
5. Bueche F. Molecular basis for the Mullins effect. *J Appl Polym Sci* 1960; 4: 107–114.
6. Diani J, Fayolle B and Gilormini P. A review on the Mullins effect. *Eur Polym J* 2009; 45: 601–612.
7. Ramier J, Gauthier C, Chazeau L, et al. Payne effect in silica-filled styrene–butadiene rubber: influence of surface treatment. *J Polym Sci Part B Polym Phys* 2007; 45: 286–298.
8. Payne AR. The dynamic properties of carbon black-loaded natural rubber vulcanizates. Part I. *J Appl Polym Sci* 1962; 6: 57–63.
9. Payne AR and Whittaker RE. Low strain dynamic properties of filled rubbers. *Rubber Chem Technol* 1971; 44: 440–478.
10. Chazeau L, Brown JD, Yanyo LC, et al. Modulus recovery kinetics and other insights into the Payne effect for filled elastomers. *Polym Compos* 21: 202–222.
11. Wang X and Robertson CG. Memory of prior dynamic strain history in filled rubbers. *Rubber Chem Technol* 2010; 83: 149–159.
12. Ogden RW and Roxburgh DG. A pseudo–elastic model for the Mullins effect in filled rubber. *Proc R Soc Lond Math Phys Eng Sci* 1999; 455: 2861–2877.
13. Gent AN and Hindi M. Effect of oxygen on the tear strength of elastomers. *Rubber Chem Technol* 1990; 63: 123–134.
14. Roland CM. Network recovery from uniaxial extension: I. Elastic equilibrium. *Rubber Chem Technol* 1989; 62: 863–879.
15. Marano C, Boggio M, Cazzoni E, et al. Fracture phenomenology and toughness of filled natural rubber compounds via the pure shear test specimen. *Rubber Chem Technol* 2014; 87: 501–515.
16. Dizon ES, Hicks AE and Chirico VE. The effect of carbon black parameters on the fatigue life of filled rubber compounds. *Rubber Chem Technol* 1974; 47: 231–249.
17. Zhao J and Ghebremeskel GN. A review of some of the factors affecting fracture and fatigue in SBR and BR vulcanizates. *Rubber Chem Technol* 2001; 74: 409–427.
18. Scott G. A review of recent developments in the mechanisms of antifatigue agents. *Rubber Chem Technol* 1985; 58: 269–283.
19. Hamed GR. Effect of crosslink density on the critical flaw size of a simple elastomer. *Rubber Chem Technol* 1983; 56: 244–251.

20. Lake GJ and Lindley PB. The mechanical fatigue limit for rubber. *J Appl Polym Sci* 1965; 9: 1233–1251.
21. Chun H and Gent AN. Strength of sulfur-linked elastomers. *Rubber Chem Technol* 1996; 69: 577–590.
22. Gent AN. Some chemical effects in fatigue cracking of vulcanized rubbers. *J Appl Polym Sci* 1962; 6: 497–502.
23. Mars WV and Fatemi A. Factors that affect the fatigue life of rubber: a literature survey. *Rubber Chem Technol* 2004; 77: 391–412.
24. Kraus G. Reinforcement of elastomers by carbon black. *Rubber Chem Technol* 1978; 51: 297–321.
25. Bergström JS and Boyce MC. Mechanical behavior of particle filled elastomers. *Rubber Chem Technol* 1999; 72: 633–656.
26. Jiang B. Do we need very stiff fillers? *Rubber Chem Technol* 2017; 90: 743–750.
27. Kahraman H and Haberstroh E. Direction-dependent and multiaxial stress-softening behavior of carbon black-filled rubber. *Rubber Chem Technol* 2014; 87: 139–151.
28. Langley NR and Polmanteer KE. Relation of elastic modulus to crosslink and entanglement concentrations in rubber networks. *J Polym Sci Polym Phys Ed* 1974; 12: 1023–1034.
29. Farlie ED. Creep and stress relaxation of natural rubber vulcanizates. Part I. Effect of crosslink density on the rate of creep in different vulcanizing systems. *J Appl Polym Sci* 1970; 14: 1127–1141.
30. Plazek DJ. Effect of crosslink density on the creep behavior of natural rubber vulcanizates. *J Polym Sci Part 2 Polym Phys* 1966; 4: 745–763.
31. Hagen R, Salmén L and Stenberg B. Effects of the type of crosslink on viscoelastic properties of natural rubber. *J Polym Sci Part B Polym Phys* 1996; 34: 1997–2006.
32. Ferry JD, Mancke RG, Maekawa E, et al. Dynamic mechanical properties of cross-linked rubbers. I. Effects of cross-link spacing in natural rubber. *J Phys Chem* 1964; 68: 3414–3418.
33. Liu R and Sancaktar E. Application of X-ray micro-CT method to assess damage/flaw presence and progression in tire rubber materials. *Proc. ASME. 57106; Volume 3: 17th International Conference on Advanced Vehicle Technologies; 12th International Conference on Design Education; 8th Frontiers in Biomedical Devices*, August 2015, V003T01A035, DETC2015-47809.
34. Liu R and Sancaktar E. Dual-stiffness behavior of fatigued tire rubber. *Proc. ASME. 57106; Volume 3: 17th International Conference on Advanced Vehicle Technologies; 12th International Conference on Design Education; 8th Frontiers in Biomedical Devices*, August 2015, V003T01A034, DETC2015-47782.
35. Liu R and Sancaktar E. Identification of crack progression in filled rubber by micro X-ray CT-scan. *Int J Fatigue* 2018; 111: 144–150.
36. Dorigato A, Dzenis Y and Pegoretti A. Filler aggregation as a reinforcement mechanism in polymer nanocomposites. *Mech Mater* 2013; 61: 79–90.